

## QUARKONIA PRODUCTION AND POLARIZATION STUDIES WITH CDF

VAIA PAPADIMITRIOU

(for the CDF Collaboration)

*Physics Department, Texas Tech University, Box 41051  
Lubbock, TX 79409, U.S.A*

In this paper we present results on production and polarization of the  $J/\psi$ ,  $\psi(2S)$ ,  $\chi_c$ ,  $\Upsilon$  and  $\chi_b$  states at  $\sqrt{s} = 1.8$  TeV. These results were obtained from data taken with the CDF detector at Fermilab. We cover recently completed analyses of the 1992-96 collider run.

### 1. Introduction

Heavy Quarkonia states,  $c\bar{c}$  and  $b\bar{b}$ , provide very useful systems for the study of both perturbative and non perturbative QCD. As far as the strong interactions are concerned, heavy quarkonia are the next simplest particles (probes) after leptons and electroweak gauge bosons. In addition, the charmonium and bottomonium systems exhibit a rich spectrum of orbital and angular excitations and therefore they can potentially provide more information than leptons and electroweak gauge bosons. The large production of heavy quarkonia in  $p\bar{p}$  colliders and the ability to trigger on them efficiently make the Tevatron a unique place for such studies allowing the disentangling of various production mechanisms.

From August 1992 to February 1996, the CDF detector collected a data sample of  $110 \text{ pb}^{-1}$  of  $p\bar{p}$  collisions at  $\sqrt{s} = 1.8$  TeV and we refer to this period as Run I. We refer to the period from 1992-93 ( $\sim 20 \text{ pb}^{-1}$ ) as Run Ia and to the period from 1994-1996 ( $\sim 90 \text{ pb}^{-1}$ ) as Run Ib. The CDF detector is described in detail elsewhere.<sup>1,2</sup> Here we describe some features of the detector, most relevant to the analyses we discuss. CDF has good tracking and lepton ID for the pseudorapidity region  $|\eta| < 1$ . The tracking system gives a transverse momentum resolution  $\delta p_T/p_T = [(0.0009 \times p_T)^2 + (0.0066)^2]^{1/2}$ , where  $p_T$  is in units of GeV/c. The average track impact parameter resolution relative to the beam axis is  $(13 + (40/p_T)) \mu\text{m}$  in the plane transverse to the beam, for  $|z| < 25$  cm, the area covered by the Silicon Vertex detector (SVX). Muon candidates consist of tracks in the central tracking chamber matched to hits in muon chambers, located outside the calorimeter. Photon candidates consist of an energy deposit in the central electromagnetic calorimeter, matched to clusters in strip chambers embedded in the calorimeter.

This paper is organized as follows. In section 2 we describe results on  $J/\psi$  and  $\psi(2S)$  production and polarization, in section 3 we describe results on  $\chi_c$  production, in section 4 we describe results on  $\Upsilon$  and  $\chi_b$  production and polarization and in

section 5 we present conclusions and discuss the future prospects.

## 2. $J/\psi$ and $\psi(2S)$ Production and Polarization

The CDF collaboration has previously reported results on the production of  $J/\psi$  and  $\psi(2S)$  mesons.<sup>3,4</sup> The measured cross sections for direct production were on the order of 50 times larger than predicted by the Color Singlet Model(CSM).<sup>5</sup> However, calculations based on the Nonrelativistic QCD (NRQCD) factorization formalism<sup>6</sup> are able to account for the observed cross sections by including color octet production mechanisms. This leads to the prediction that directly produced  $\psi$  mesons will be increasingly transversely polarized at high  $p_T$ .<sup>7,8,9</sup> (In this paper we use  $\psi$  to denote either  $J/\psi$  or  $\psi(2S)$  mesons.) This is because the production of  $\psi$  mesons with  $p_T \gg M_\psi$  is dominated by gluon fragmentation and it is predicted that the gluon's transverse polarization is preserved as the  $c\bar{c}$  pair evolves into a bound state  $\psi$  meson. On the other hand the Color Evaporation Model predicts an absence of polarization.<sup>10</sup> The data used in this study correspond to  $\sim 110 \text{ pb}^{-1}$  and were collected with the dimuon trigger. The measurement of the polarization of  $J/\psi$  and  $\psi(2S)$  mesons is made by analyzing their decays to  $\mu^+\mu^-$  in the helicity basis, in which the spin quantization axis lies along the  $\psi$  direction in the  $p\bar{p}$  center-of-mass frame. The angle  $\theta$  is given by the direction of the  $\mu^+$  in the  $\psi$  rest frame and the  $\psi$  direction in the  $p\bar{p}$  center-of-mass frame. The normalized angular distribution  $I(\theta)$  is given by  $I(\theta) = \frac{3 \cdot (1 + \alpha \cos^2 \theta)}{2(\alpha + 3)}$ . Unpolarized  $\psi$  mesons have  $\alpha = 0$  while  $\alpha = +1$  or  $-1$  correspond to fully transverse or longitudinal polarizations respectively.

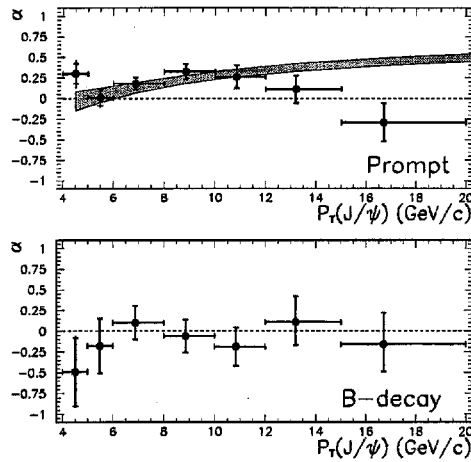


Fig. 1. The fitted polarization of  $J/\psi$  mesons from prompt production and  $B$ -hadron decay, in seven  $p_T$  bins, for  $|y^{J/\psi}| < 0.6$ . The shaded band shows an NRQCD factorization prediction<sup>9</sup> which includes the contribution from  $\chi_c$  and  $\psi(2S)$  decays.

Our method of determining  $\alpha$  is to fit the observed distributions of  $\cos\theta$  to distributions derived from simulated  $\psi \rightarrow \mu^+\mu^-$  decays. In order to extract the polarization parameter  $\alpha$  for promptly produced  $\psi$  mesons, we separate the prompt component ( $\alpha_P$ ) from the  $B$ -decay component ( $\alpha_B$ ) using the proper decay length of each event. The  $J/\psi$  polarization is measured in seven  $p_T$  bins covering the range 4-20 GeV/c. In fig. 1 we show our fit results for  $\alpha_P$  and  $\alpha_B$  and we compare  $\alpha_P$  with a theoretical NRQCD prediction.<sup>9</sup> The measurement of the  $\psi(2S)$  polarization is measured in three  $p_T$  bins covering the region 5.5-20.0 GeV/c. The fitted values for  $\alpha_P$  and  $\alpha_B$  as a function of  $P_T^{\psi(2S)}$  are shown in fig. 2 together with two NRQCD predictions. The polarization from  $B$  decays ( $\alpha_B$ ) is generally consistent with zero, as expected. In both the  $J/\psi$  and  $\psi(2S)$  states, we do not observe increasing prompt transverse polarization for  $p_T \geq 12$  GeV/c, in disagreement with NRQCD factorization predictions.<sup>8,9</sup>

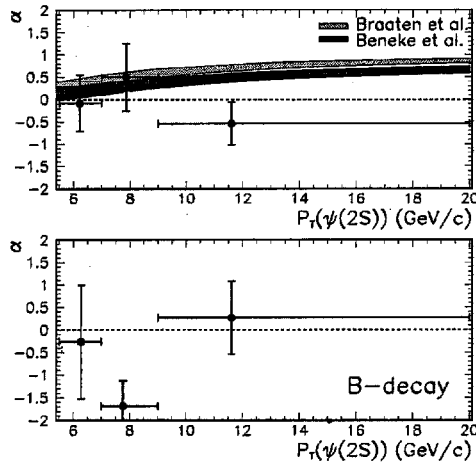


Fig. 2. The fitted polarization of  $\psi(2S)$  mesons from prompt production and  $B$ -hadron decay, in three  $p_T$  bins, for  $|\eta^{\psi(2S)}| < 0.6$ . The prompt polarization is compared with two NRQCD factorization predictions.<sup>8,9</sup>

### 3. $\chi_c$

Using  $\sim 18 \text{ pb}^{-1}$  of data from Run Ia we studied<sup>4</sup> the reaction  $p\bar{p} \rightarrow \chi_c X$ ;  $\chi_c \rightarrow J/\psi\gamma$  and have identified  $1230 \pm 72$   $\chi_c$  signal events. For  $p_T(J/\psi) > 4.0$  GeV/c and  $|\eta(J/\psi)| < 0.6$  we have measured the fraction of  $J/\psi$  mesons originating from  $\chi_c$  meson decays to be  $29.7 \pm 1.7(\text{stat}) \pm 5.7(\text{sys})\%$ , not including contributions from  $b$  hadrons. This fraction is approximately independent of  $p_T^{J/\psi}$  between 4 and 15 GeV/c. We have also found that the fraction of prompt  $J/\psi$ 's from  $\psi(2S)$ 's rises from  $7 \pm 2\%$  at  $p_T^{J/\psi} = 5$  GeV/c to  $15 \pm 5\%$  at  $p_T^{J/\psi} = 18$  GeV/c. The fraction of

directly produced  $J/\psi$ 's is  $64 \pm 6\%$  and it is approximately independent of  $p_T^{J/\psi}$  between 5 and 18 GeV/c. Direct production is therefore the largest source of prompt  $J/\psi$  mesons. We used the above fraction measurements to subtract from the prompt  $J/\psi$  cross section the contribution from  $\chi_c$  and  $\psi(2S)$  decays and derive the direct  $J/\psi$  differential cross section discussed in the previous section. Using  $\sim 110 \text{ pb}^{-1}$

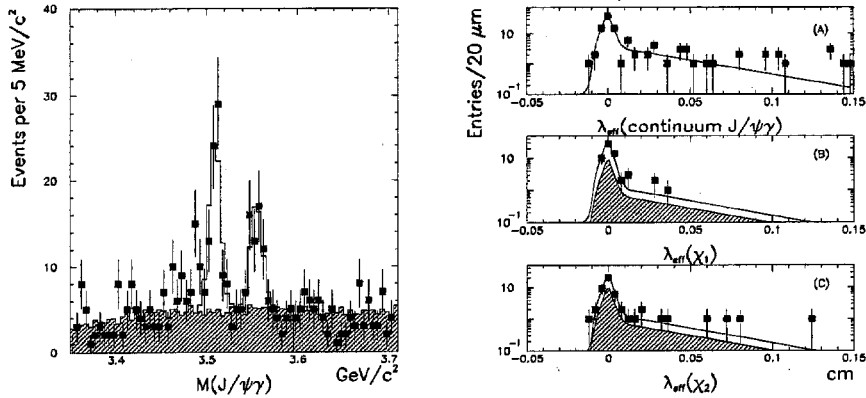


Fig. 3. (left) The  $J/\psi\gamma$  mass spectrum. The background estimate is indicated by the shaded area, and the solid histogram shows the result of the likelihood fit for the  $\chi_{cJ}$  signals. (right) The  $J/\psi\gamma$  effective decay length spectrum for events measured in the SVX. (A) The decay length distribution for candidates having  $3350 \text{ MeV}/c^2 < M(J/\psi\gamma) < 3470 \text{ MeV}/c^2$  and  $3590 \text{ MeV}/c^2 < M(J/\psi\gamma) < 3710 \text{ MeV}/c^2$ . (B) The decay length distribution for the  $\chi_{c1}$ ,  $3492 \text{ MeV}/c^2 < M(J/\psi\gamma) < 3528 \text{ MeV}/c^2$ . (C) The decay length distribution for the  $\chi_{c2}$ ,  $3538 \text{ MeV}/c^2 < M(J/\psi\gamma) < 3574 \text{ MeV}/c^2$ . The fit to the data points is shown in each distribution. The shaded functions in (B,C) indicate the effective decay length distribution due to background sources.

of data, we have also measured the relative rate of production of the charmonium states  $\chi_{c1}$  and  $\chi_{c2}$  through their decay into  $J/\psi\gamma$ . The photon from the decay is reconstructed here through conversion into  $e^+e^-$  pairs, which makes the resolution of the two states possible. The effective lifetime ( $\lambda_{eff}$ ) is used to discriminate between  $\chi_c$  events produced promptly and through  $B$  decay processes. The predominant  $\chi_{cJ}$  background is believed to be due to photons resulting from the decay of  $\pi^0$ ,  $\eta$  and  $K_S^0$  produced in association with the  $J/\psi$ . Although the existence of the process is poorly established, we nonetheless consider a second source of background due to the partial reconstruction of  $h_c(1P) \rightarrow J/\psi\pi^0; \pi^0 \rightarrow \gamma\gamma$ . The  $J/\psi\gamma$  mass spectrum is shown in fig. 3, left. The  $\chi_{c1}$  and  $\chi_{c2}$  are clearly resolved, although no evidence for the  $\chi_{c0}$  is seen in this distribution. The effective decay length distribution for events measured in the SVX is shown in fig. 3, right. The mass and decay length distributions are fit simultaneously using the maximum likelihood method to obtain the number of  $\chi_{c1}$  and  $\chi_{c2}$  events due to prompt production. The fit gives  $118.7 \pm 13.5$  total  $\chi_{cJ}$ . The ratio of events between the  $\chi_{c1}$  and  $\chi_{c2}$  is measured to be  $N_{\chi_{c2}}/N_{\chi_{c1}} = 0.65 \pm 0.15$  for the full data sample and  $0.56 \pm 0.16$  in the

prompt subset of the data. We find the ratio of production cross sections  $\frac{\sigma_{\chi_{c2}}}{\sigma_{\chi_{c1}}} = 0.96 \pm 0.27(\text{stat}) \pm 0.11(\text{sys})$  for events with  $p_T(J/\psi) > 4.0$  GeV/c,  $|\eta(J/\psi)| < 0.6$  and  $p_T(\gamma) > 1.0$  GeV/c. A recent NRQCD prediction<sup>11</sup> for the cross section ratio is equal to  $1.1 \pm 0.2$ , in good agreement with this measurement.

#### 4. $\Upsilon$ 's and $\chi_b$ 's

Using  $\sim 77$  pb<sup>-1</sup> of dimuon trigger data from Run Ib we identify  $4430 \pm 95$   $\Upsilon(1S)$  events,  $1114 \pm 65$   $\Upsilon(2S)$  events and  $584 \pm 53$   $\Upsilon(3S)$  events in the rapidity region  $|y(\Upsilon)| < 0.4$  and for  $0$  GeV/c  $< p_T(\Upsilon) < 20$  GeV/c. The  $\Upsilon$  mass distributions are then fitted as a function of the dimuon  $p_T$  in order to extract differential cross sections. These cross sections are higher than CSM predictions<sup>12</sup> by factors between 3-5 for  $p_T^{\Upsilon} > 3$  GeV/c. The  $p_T$  shape cannot be reproduced by CSM in the  $p_T^{\Upsilon} < 3$  GeV/c region.

Using  $\sim 90$  pb<sup>-1</sup> of data from Run Ib we have also searched for the radiative decays of  $\chi_b$  and see evidence for  $\chi_b(1P) \rightarrow \Upsilon(1S)\gamma$  and  $\chi_b(2P) \rightarrow \Upsilon(1S)\gamma$  for relatively high  $p_T^{\Upsilon(1S)}$ .  $\Upsilon(1S)$  candidates with  $p_T > 8$  GeV/c ( $1462 \pm 55$  events) are combined with photon candidates with energy greater than 0.7 GeV. We show the  $\Delta M = M(\mu^+\mu^-\gamma) - M(\mu^+\mu^-)$  mass distribution in fig. 4. The number of  $\chi_b$  signal events is determined by fitting the data  $\Delta M$  distribution to the sum of the background distribution and two gaussian functions associated with the signals. The fit results in  $35.3 \pm 9.0$  and  $28.5 \pm 12.0$  signal events for  $\chi_b(1P)$  and  $\chi_b(2P)$  respectively. We have measured the fractions of  $\Upsilon(1S)$  mesons originating from  $\chi_b(1P)$ ,  $\chi_b(2P)$  and  $\chi_b(3P)$  decays to be  $27.1 \pm 6.9(\text{stat}) \pm 4.4(\text{sys})\%$ ,  $10.5 \pm 4.4(\text{stat}) \pm 1.4(\text{sys})\%$  and less than 6% respectively for  $p_T^{\Upsilon(1S)} > 8$  GeV/c. For the same kinematic region we have also found that the fractions of  $\Upsilon(1S)$  mesons originating from  $\Upsilon(2S)$  and  $\Upsilon(3S)$  mesons are  $10.7^{+7.7}_{-4.8}\%$  and  $0.8^{+0.6}_{-0.4}\%$  respectively. The fraction of directly produced  $\Upsilon(1S)$  mesons was measured to be  $50.9 \pm 8.2(\text{stat}) \pm 9.0(\text{sys})\%$ .

We have also performed a polarization analysis on the  $\Upsilon(1S)$  data sample in a similar way to that on the  $\psi$  sample. We study again the angle  $\theta$  given by the direction of the  $\mu^+$  in the  $\Upsilon(1S)$  rest frame and the  $\Upsilon$  direction in the  $p\bar{p}$  center-of-mass frame. Here we do not have the complication of having to separate the prompt decays from the  $B$  decays. In the range  $2 < p_T < 20$  GeV/c the fitted longitudinal fraction is  $\Gamma_L/\Gamma = 0.37 \pm 0.04$ , corresponding to an  $\alpha$  of  $-0.08 \pm 0.09$ , consistent with unpolarized  $\Upsilon$ 's. In the more restricted range  $8 < p_T < 20$  GeV/c the fitted fraction is  $\Gamma_L/\Gamma = 0.32 \pm 0.11$  corresponding to an  $\alpha$  of  $0.03 \pm 0.25$ , again consistent with unpolarized  $\Upsilon$ 's. This result does not contradict predictions including color octet mechanisms since transverse polarization is expected to be large only for  $p_T \gg M_{\Upsilon}$ .

#### 5. Conclusions-Prospects

In this paper we have presented results on Quarkonia production as well as on Quarkonia Polarization. The Quarkonia cross sections are higher than the theoret-

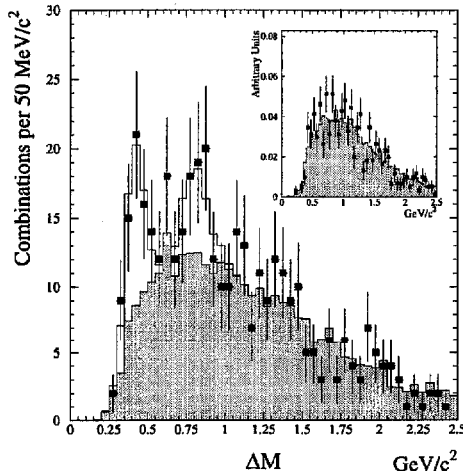


Fig. 4. The  $\Delta M = M(\mu^+\mu^-\gamma) - M(\mu^+\mu^-)$  distribution. The points represent the data. The shaded histogram is the background shape predicted by the Monte Carlo calculation. The solid line is the fit of the data to two gaussian functions plus the background histogram. The inset shows the comparison between the  $\Delta M$  distribution for dimuons in the  $\Upsilon(1S)$  sidebands and the corresponding one predicted by the Monte Carlo calculation.

ical expectations. The polarization of the  $J/\psi$  and  $\psi(2S)$  mesons does not increase as a function of the  $\psi$   $p_T$ , in disagreement with NRQCD factorization predictions. We have measured the fractions of  $J/\psi$  originating from other charmonia states or produced directly and the fractions of  $\Upsilon(1S)$  produced from other botommonia states or produced directly. We measured the ratio of  $\chi_{c2}$  over  $\chi_{c1}$  cross sections to be consistent with NRQCD theoretical expectations.

The Tevatron will commence  $p\bar{p}$  collisions again at  $\sqrt{s} = 2.0$  TeV in March of 2001 with an initial goal of delivering an integrated luminosity of  $1 \text{ fb}^{-1}$  per year, corresponding to approximately  $10^{11}$   $b\bar{b}$  pairs produced per year. This upcoming data taking period is referred to as Run II. We expect to collect a data sample of more than  $15 \cdot \text{fb}^{-1}$  before 2007 which will allow us to further investigate and shed more light on the Charm, Beauty and Quarkonia production and polarization mechanisms.

### Acknowledgements

We thank the Fermilab staff and the technical staffs of the participating institutions for their vital contributions. This work was supported by the U.S. Department of Energy and National Science Foundation; the Italian Istituto Nazionale di Fisica Nucleare; the Ministry of Education, Science and Culture of Japan; the Natural Sciences and Engineering Research Council of Canada; the National Science Council

of the Republic of China; and the A. P. Sloan Foundation.

## References

1. F. Abe *et al.*, Nucl. Instrum. Methods **A271** 387 (1988).
2. F. Abe *et al.*, Phys. Rev. **D50**, 2966 (1994).
3. F. Abe *et al.*, Phys. Rev. Lett. **79**, 572 (1997).
4. F. Abe *et al.*, Phys. Rev. Lett. **79**, 578 (1997).
5. M. Cacciari, M. Greco, Phys. Rev. Lett. **73**, 1586 (1994); E. Braaten *et al.*, Phys. Lett. **B333**, 548 (1994); D.P. Roy and K. Sridhar, Phys. Lett. **B339**, 141 (1994).
6. G. Bodwin, E. Braaten and G. Lepage, Phys. Rev. **D51**, 1125 (1995) (Erratum *ibid.* **55**, 5853 (1997)); E. Braaten and S. Fleming, Phys. Rev. Lett. **74**, 3327 (1995); M. Cacciari *et al.*, Phys. Lett. **B356**, 553 (1995); E. Braaten and Y. Chen, Phys. Rev. **D54**, 3216 (1996); P. Cho and A.K. Leibovich, Phys. Rev. **D53**, 150, (1996), P. Cho and A.K. Leibovich, Phys. Rev. **D53**, 6203 (1996).
7. P. Cho and M. Wise, Phys. Lett. **B346**, 129 (1995).
8. M. Beneke and M. Kramer, Phys. Rev. **D55**, 5269 (1997).
9. E. Braaten, B. Kniehl and J. Lee, hep-ph/9911436.
10. J. Amundson *et al.*, Phys. Lett. **B390**, 323 (1997).
11. F. Maltoni, private communication. Work based on<sup>6</sup>.
12. A. Leibovich, private communication. Work based on<sup>5</sup>.